Semi-empirical model for indirect measurement of soot size distributions in compression ignition engines

Francisco, Martos; Martin-Gonzalez, Gema; Herreros, Jose

DOI:
10.1016/j.measurement.2018.03.081

Document Version
Peer reviewed version

Citation for published version (Harvard):
Francisco, M, Martin-Gonzalez, G & Herreros, J 2018, 'Semi-empirical model for indirect measurement of soot size distributions in compression ignition engines', *Measurement*, vol. 124, pp. 32-39. https://doi.org/10.1016/j.measurement.2018.03.081

Semi-empirical model for indirect measurement of soot size distributions in compression ignition engines

Martos, F.J.,[a,*], Martín-González, G.[a], Herreros, J.M.[b]

[a]*Escuela de Ingenierías Industriales, University of Málaga, c/Doctor Ortiz Ramos, s/n, 29071, Málaga, Spain*
[b]*School of Mechanical Engineering, University of Birmingham, Edgbaston, B15 2TT, UK*

Abstract

This work proposes a semi-empirical model, which provides soot particle size distribution functions emitted by compression ignition engines. The model is composed of a phenomenological model based on the collision dynamics of particle agglomerates and an empirical model, which provides key input parameters such as primary particle size and a mathematical relationship between the size of the agglomerate and number of primary particles. The phenomenological model considers the relevant fluid-dynamics phenomena influencing the collision frequency function. It is observed that Brownian motion is the predominant phenomenon and in a much lesser degree inertial turbulent motion. The experimental model requires air/fuel ratio, engine speed, soot density and mean instantaneous in-cylinder pressure. A Dirac delta is used as a seed for the agglomerate size function whose magnitude depends on the soot volume concentration and the mean primary particle size at each engine operation condition. In a further step, the obtained modelled agglomerate size functions are fitted to lognormal size distributions defined by the modelled mean size and standard deviation. Modelled lognormal agglomerate size distribution functions are validated with respect to experimental distributions obtained using a Scanning Mobility Particle Sizer (SMPS).

Keywords: particle size distribution function, soot, compression ignition engines, semi-empirical modelling

*Corresponding author
Email address: fjmartos@uma.es (Martos, F.J.,)

1. Introduction

Compression ignition engines have significant advantages in terms of engine performance, fuel economy and CO_2 emissions compared to spark ignition engines. However, they have the drawback of high NO_x and particulate matter (PM) emissions derived from their non-homogeneous combustion process. Regulatory actions aiming to mitigate the environmental [1] and public health [2] effects of particulate matter released by vehicles have been put in place. The mass of PM emissions has been regulated in Europe since Euro 1 in light duty passenger cars and commercial vehicles powered by diesel engines. Particle size affects (i) particle reactivity through the surface/volume ratio, (ii) particle suspension time in the atmosphere and (iii) particle trapping efficiency in a filtration system, and thus the environmental and health effects of particles. As a result, since the entry into force in Europe of Euro 5b in September 2011 [3], not only the mass emissions of particles are regulated but also the total number of particles for both diesel and gasoline powered vehicles. It could be also evaluated the possibility to introduce the particle size as a limitation factor in the future.

Particles are formed in locally rich-in-fuel regions in the combustion chamber. Fuel molecules which do not have access to oxygen are pyrolysed producing aromatics and other hydrocarbon species (such as C_2H_2, C_2H_4, C_3H_6, C_4H_4), which can act as polycyclic aromatic hydrocarbons (PAHs) and soot precursors. PAHs from a certain size condense forming a 1-2 nm nuclei (nucleation). Those nuclei undergoes surface growth maintaining a quasi-spherical shape [4, 5] while increasing the C/H ratio forming the so-called primary particles with sizes between 15 and 30 nm depending on fuel, engine and engine operation condition. Thereafter, particle agglomerates are formed as a consequence of collisions between the primary particles and/or primary particles and agglomerates. The formed agglomerates loose the spherical shape becoming like-fractal structures [6, 7], thus equivalent diameters based on different properties are defined to quantify agglomerate size. Equivalent diameter of a non-spherical particle is

the diameter of a spherical particle that gives the same value of a specific property (aerodynamic, electrical mobility, optical, etc.) to that of the non-spherical agglomerate. For instance, electrical mobility diameter can be related by potential functions with other characteristic sizes such as the radius of gyration [8, 9].

The determination of particle size distribution functions not only provides information related to the environmental and human health effects but also could contribute to the diagnosis of the causes of particle formation as well as to adopt actions for their abatement. Exhaust particle size distributions are measured using particle sizer spectrometers such as Scanning Mobility Particle Sizer (SMPS) [10], Engine Exhaust Particle Spectrometer (EEPS), Cambustion DMS 500 [11], Electrical Low Pressure Impactor (ELPI) [12], etc. These equipment require the dilution of the exhaust to reproduce atmospheric conditions and adapt the sample in temperature and particle concentration to be measured by the equipment. Thus, this process could provoke quantitative and qualitative differences to the agglomerate size distribution [13]. The modeling of size distribution functions has been studied in [14] for generic aerosols or in works as [15], [16] and [17] for soot aerosols. The complex nature of pollutant formation and oxidation in compression ignition engines [18] and [19] results in the utilisation of different types of models and/or their combination including phenomenological (physically motivated relations), empirical (measured data to identify the relations) [20] and hybrid approaches combining physical and empirical relations (semi-empirical models) [21]. Phenomenological and empirical approaches both have appropriate characteristics but also present disadvantages. Phenomenological models predict qualitative trends but the physically motivated relations are difficult to identify [22] and [23] and have limitations from error propagation and computational time [24]. On the other hand, empirical models are computational efficient, fit accurately to quantitative measurement results and are simple to handle, [25]. The major limitation of empirical models is the lack of reliable extrapolation beyond the conditions where the model is fitted and that only the parameters explicitly present in the model could be identified. Semi-empirical

models combine the capabilities of physical models providing reliable qualitative trends enabling the model extrapolation with minimum number of constraints and measurements required to adjust the model as well as the computational efficiency of empirical models [21].

This paper aims to develop a new methodology to estimate the size distribution function of the soot agglomerates emitted from compression ignition engines using a semi-empirical model composed of a phenomenological and empirical model. The model is validated with respect to agglomerate size distribution experimentally measured using an SMPS in the same engine operation conditions. Section 2 describes the proposed semi-empirical model including the hypotheses, phenomenological dynamics of the collisions between agglomerates, and the relations between agglomerate size and number of primary particles. The experimental facilities and techniques used to obtain the input of the model (e.g. in-cylinder pressure, engine speed, Air/Fuel ratio, and volumetric soot concentration) are presented in Section 3. The experimental particle size distributions and model validation are developed in Section 4, while conclusions are presented in Section 5.

2. Methodology and experimental installation

The proposed semi-empirical model provides particle size distributions for different engine operation conditions requiring instantaneous in-cylinder pressure, total volumetric soot concentration, engine speed and Air/Fuel ratio as inputs. The obtained particle size distributions are in the nanometric range. The model is composed of a phenomenological model to describe particle collisions in the combustion chamber, as well as empirical models which feed the phenomenological model (see figure 1). Particularly, the empirical model provides the relationship between the initial primary particle size and engine operation condition (engine speed, Air/Fuel ratio) as well as the correlation between the number of primary particles per agglomerate and agglomerate size. The resultant agglomerate size distribution is fitted to a log-normal distribution function

maintaining the mode and standard deviation. The results of the semi-empirical model are validated with respect to experimental agglomerate size distributions measured using an SMPS in the same engine operation conditions.

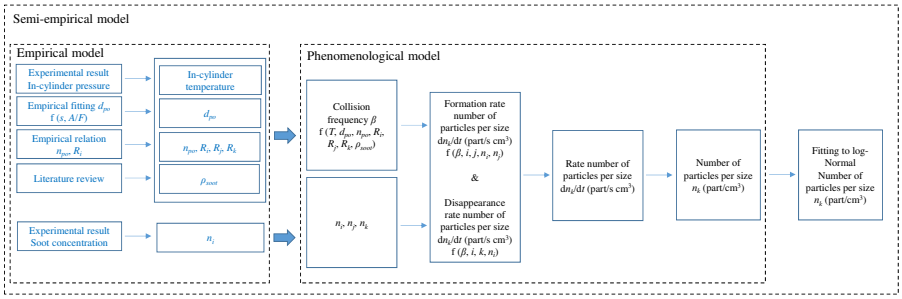

Figure 1: Scheme of the semi-empirical model

The experimental tests to obtain the required model input parameters and the results to validate the model have been carried out in a Nissan YD2.2 turbocharged compression ignition engine operated by standard EN590 diesel fuel. An asynchronous brake, Schenck brand Dynas III LI 250 has been used to provide to the engine the desired operation load. Soot concentration produced by the engine is measured with an AVL 415 smokemeter. The instantaneous mean in-cylinder pressure values have been measured using a Kistler piezoelectric transducer model Z17090sp149. The crankshaft rotation angle has been measured with an optical angle encoder AVL364. These two signals have been synchronized by a Yokogawa OR1400 oscilloscope. From the instantaneous mean in-cylinder pressure and by using a zero-dimensional thermodynamic model within the combustion chamber, [26, 27], the instantaneous mean temperature inside the combustion chamber can be obtained. A SMPS has been used to measure the particle size distribution function in the tailpipe to validate the semi-empirical model. The SMPS classifies the particles according to their mobility size. The SMPS used is from TSI, model 3936L10, and the particle counter is CPC model 3010S. The Differential Mobility Analyzer (DMA) has a sizing uncertainty of approximately $3 - 3.5\%$, [28]. The SMPS has a particle

size measurement range from 10 to 500 nm.

A reference engine operation condition extracted from the urban driving of the light vehicle type-approval cycle has been chosen. This point has been denoted as L2. The engine load has been varied at this operating point, keeping the rest of the engine's operating parameters constant, such as the engine speed maintained at 1525 rpm and EGR (0% EGR). The five engine test points are summarised in the table 1, including torque, Air/Fuel ratio, brake mean effective pressure (BMEP) and the soot concentration, while the instantaneous in-cylinder temperature is shown in Figure 2. The starting point for the model has been located when the combustion starts in the combustion chamber, and has been denoted as t_0.

Operating mode	Torque (Nm)	Air/Fuel ratio	BMEP (bar)	C ($mg \cdot m^{-3}$)
L1	27.2	43.00	1.53	11.42
L2	45.4	32.28	2.63	16.25
L3	58.4	26.99	3.36	21.67
L4	70.8	23.37	4.08	62.20
L5	83.1	20.05	4.80	348.86

Table 1: Engine operating conditions.

3. Proposed model

The semi-empirical model solves the equations that express the balance of the number of particles per size of a distribution function. The size distribution is discretized in terms of the particle collision frequency to which is subjected an initial mono-disperse population of primary particles under Brownian movement [29].

3.1. Assumptions

1. Initially the aerosol is monodisperse. The aerosol considered at the beginning of the simulation is monodisperse being composed of solid spherical

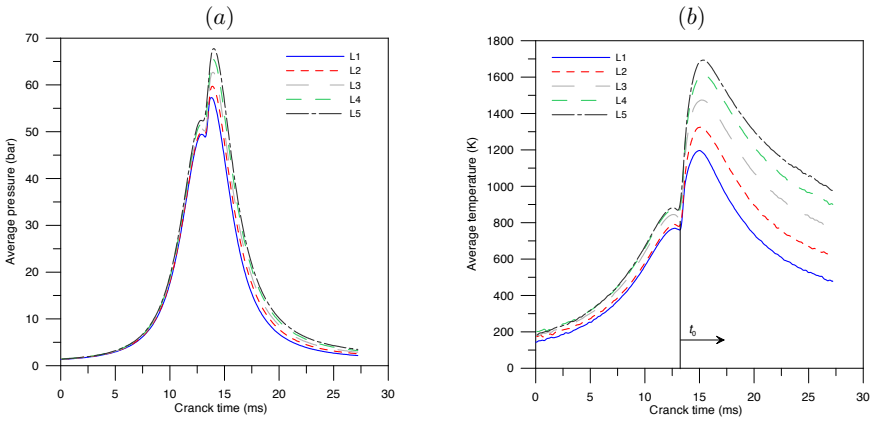

Figure 2: Average pressure (a) and average temperature (b) inside the combustion chamber vs. crank time.

primary particles in suspension, with a diameter d_{po}.

2. Conservation of mass. The mass of the particle formed after a collision is equal to the sum of the masses of the particles that collided.
3. Loss of identity of colliding particles. The particle formed after a collision of two particles has different fractal dimension to its progenitors, [30].
4. Instantaneous internal coalescence time. The collision and recombination processes to form the new particle is instantaneous.

3.2. Collision dynamics of particle agglomerates

The particle number concentration at size k (n_k) is obtained as the balance between the formation of new particles and the disappearance of particles of size k. Both of them are dependent from the number of particle collisions (N). The number of collisions between particles at size i and j can be calculated considering the frequency of particle collision (β_{ij}) and the concentration of particles at size i and j being mathematically expressed in equation (1).

$$N_{ij} = \beta\,(i,j)\,n_i n_j, \tag{1}$$

where $\beta(i,j)$ is the function of the collision frequency that depends on the size of the colliding particles and the gas properties (see further mathematical details in reference [31]), while n_i and n_j are the concentration of particles of size i and j per unit of volume.

Taking into consideration equation (1), the net rate of particles (formation/disappearance) per particle size k at a given instant can be calculated (2). Therefore, the number of particles per particle size (agglomerate size distribution) leaving the engine combustion chamber could be obtained from integration of Equation (2) assuming mass conservation and instantaneous internal coalescence time. It has to be noted that the particle formation rate for size k, $(k = i + j)$, must be affected by a factor of $\frac{1}{2}$ in order to avoid duplication in formation.

$$\frac{\mathrm{d}n_k}{\mathrm{d}t} = \frac{1}{2}\sum\nolimits_{i+j=k} \beta(i,j)\, n_i n_j - n_k \sum\nolimits_{i=1}^{\infty} \beta(i,k)\, n_i \tag{2}$$

As commented above, the collision frequency function $\beta(i,j)$ depends on the number and characteristics of the particles involved in such collisions and the gas properties. Basically, there are two main mechanisms into a combustion chamber to drive the collisions: Brownian movement and inertial movement due to fluid turbulence. In the case under study, the inertial movement can be neglected in a first approximation. To show that, it is known that the characteristic scale of a soot agglomerate is $d_p \sim 100$ nm, [30]. On the other hand, at the Kolmogorov scale η viscosity dominates and the turbulent kinetic energy is dissipated into heat, being negligible the inertial movement. In other words, η is a measure of the size of eddies at which molecular viscosity becomes dominant. An estimate for the ratio of the largest L to smallest η length scales in turbulent flows is given in equation (3), [32].

$$\frac{L}{\eta} \sim \left(\frac{UL}{\nu}\right)^{3/4} = Re^{3/4}, \tag{3}$$

where Re, is the Reynolds number based on the large scale flow features, U is a characteristic velocity and L is a characteristic length, and ν, the kinematic

viscosity of the gas. For the engine under study, we can choose: as characteristic length the diameter of the cylinder $L \sim D = 86.5 \times 10^{-3}$ m; as characteristic velocity the mean piston speed, $U = 2 \times stroke \times n/60$, that for $n = 1525$ rpm and $stroke = 94 \times 10^{-3}$ m it is found $U = 4.78$ m/s; finally, for an average temperature inside the chamber of 1500 K and a pressure of 70 bar, the kinematic viscosity of the air is $\nu \sim 3.5 \times 10^{-6}\, m^2/s$. Thus, the Reynolds number for the large scales is $Re \sim 1.2 \times 10^5$. Therefore, Eq. 3 yields,

$$\eta \sim \frac{L}{Re^{3/4}} \sim 13.6 \times 10^{-6}\ \text{m} = 13.6\ \mu\text{m}, \tag{4}$$

which is the typical value for the Kolmogorov scale found in other studies [33]. In summary, since $\eta/d_p \sim 140$, the inertial movement can be neglected versus the Brownian movement in the collision frequency function $\beta\,(i,j)$ for soot particles.

As collision frequency is dominated by Brownian motion and the aerosol could be considered discreet (Knudsen number greater than 10), the function of collision frequency is obtained from the kinetic theory of gases, [31] and [34].

$$\beta(i,j) = \left(\frac{3\pi KT}{\rho_s d_{po}^3}\right)^{\frac{1}{2}} (R_i + R_j)^2 \left(\frac{1}{n_{po,i}} + \frac{1}{n_{po,j}}\right)^{\frac{1}{2}} \tag{5}$$

where R_i and R_j are radii of the sphere that circumscribes to the particles at size i and j respectively, $n_{po,i}$ and $n_{po,j}$ are the number of primary particles contained in the agglomerates at size i and j, $K = 1.3807 \cdot 10^{-23}$ (J/K) is Boltzmann's constant, T is the average temperature within the combustion chamber determined with a zero dimensional three zone thermodynamics models, [35], ρ_s is the density of soot, which in this case has been taken a value of 1850 (kg/m^3), [36] and d_{po} is the average diameter of the primary particles that make up the agglomerate, which depends on engine speed (s) and the ratio of fresh air inducted by the engine and fuel consumed (A/F), calculated according to [36].

$$d_{po}(\text{nm}) = 50.6 - 18.9\frac{s}{2000} - 10.3\frac{A/F}{30} \tag{6}$$

As it can be seen in equation (5), the number and size of primary particles and the size of the agglomerates are unknow to calculate the collision frequency.

Therefore, a relationship between the number of primary particles and the agglomerate size is proposed in the following section.

3.3. Relationship between the agglomerate size and number of primary particles

Synthetic agglomerates have been generated in order to find a correlation between the agglomerate size and the number of primary particles. The algorithm to simulate the synthetic agglomerates based on random cluster-cluster collisions has been developed by the authors and further details can be found in Martos *et al.* [30]. A representative example of the simulated agglomerates is shown in Figure 3(b). For comparison purposes, Figure 3(a) shows a picture taken with a High Resolution Transmission Electron Microscope (HR-TEM) of a real particle agglomerate originated within a combustion chamber of a compression ignition engine. The particle was collected using the experimental technique based on the thermophoretic phenomenon reported in [36] (see further details in Lapuerta *et al.* [36]).

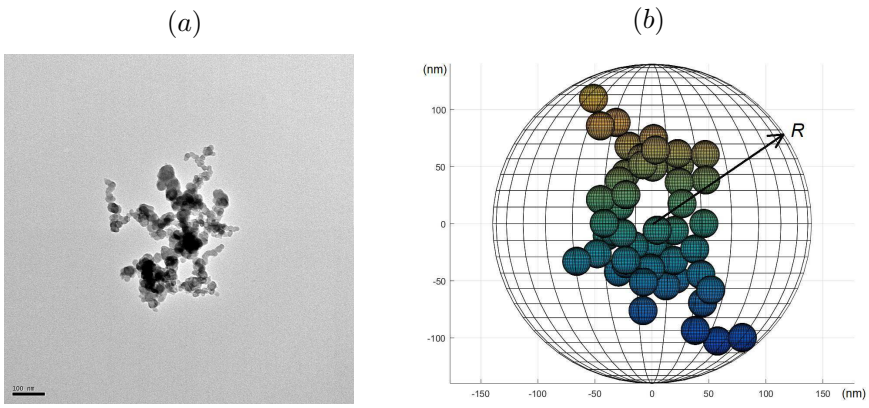

Figure 3: Views of a real agglomerate (a) and a synthetic agglomerate (b).

In order to find an appropiate correlation between the radius R and the number of primary particles n_{po}, 250000 synthetic agglomerates were simulated (gray circles) being n_{po} random. However, for the sake of clarity only 10000 sim-

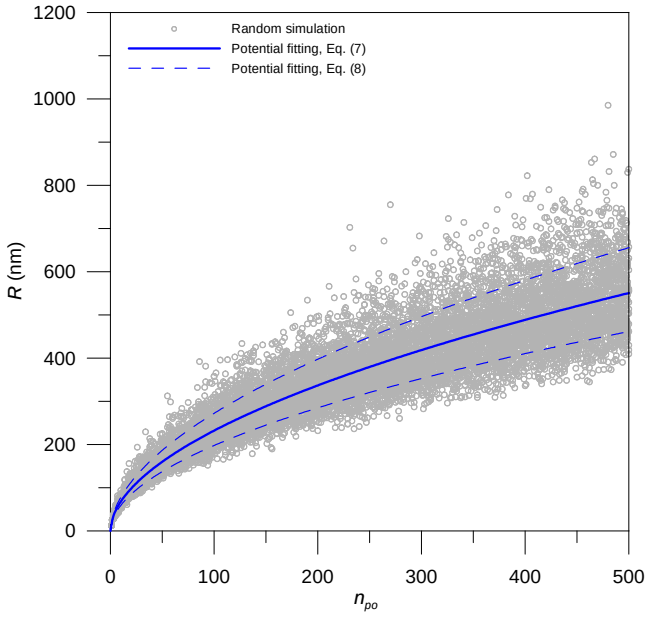

Figure 4: Random simulations (circles) and least-squares fittings (lines).

ulations have been plotted in Fig. 4 (one every 25 simulations). The blue solid line in Figure 4 corresponds to the potential fitting for the 250000 agglomerates,

$$\frac{\overline{R}}{d_{po}} = 0.7831\, n_{po}^{0.5369}, R^2 = 0.9146, \tag{7}$$

being the validity of the fitting for $n_{po} \leq 500$.

To show that R follows a normal distribution function, the results for 500 random simulations, keeping constant n_{po} for four characteristic sizes of agglomerates, have been included in Fig. 5: small size (a) $n_{po} = 50$; intermediate sizes (b) $n_{po} = 100$ and (c) $n_{po} = 200$; large size (d) $n_{po} = 300$. Since the population for each n_{po} is higher than 50, the assumption of normality can be checked using the test of Kolmogorov-Smirnov with the correction of Lilliefors.

As can be appreciated in Fig. 5, the distribution functions follow a Gaussian distribution, with mean $\overline{R}$ and standard deviation σ. Therefore, the radius of the synthetic agglomerate will fall into the interval $\overline{R} - \sigma < R < \overline{R} + \sigma$ with

$\sim 68.27\%$ probability. This interval is plotted in Fig. 4 with dashed-lines, being the fittings,

$$\begin{cases} \frac{\overline{R}_{+\sigma}}{d_{po}} = 0.8789\, n_{po}^{0.5464}, R^2 = 0.9947, \\ \frac{\overline{R}_{-\sigma}}{d_{po}} = 0.6984\, n_{po}^{0.5269}, R^2 = 0.9975. \end{cases} \tag{8}$$

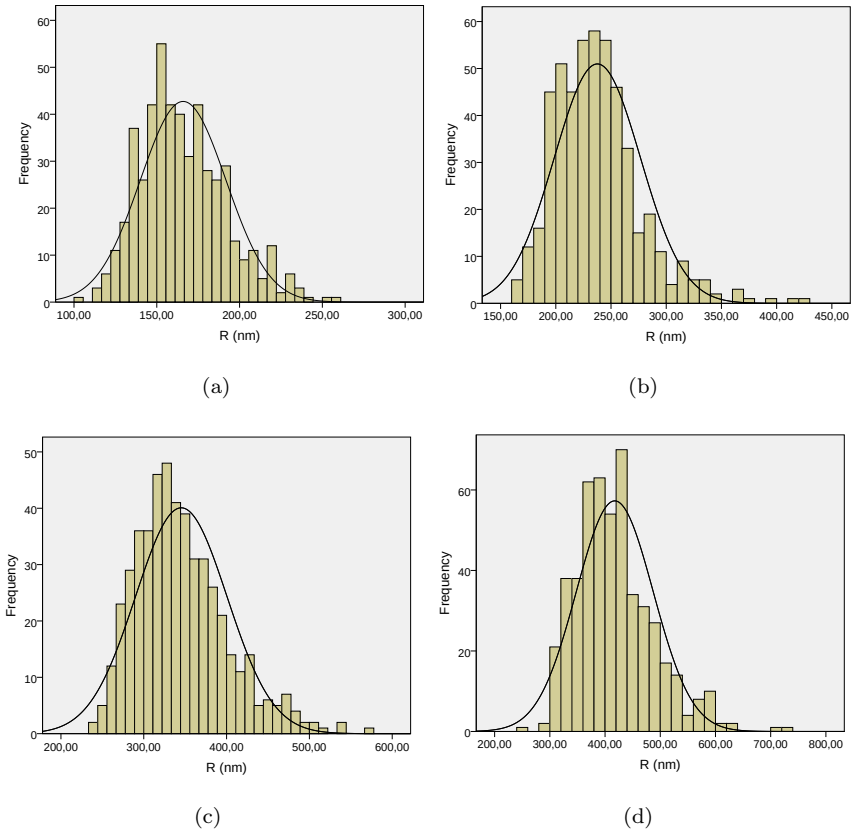

Figure 5: Number of agglomerates versus radius, keeping constant the number of primary particles that compose them. (a) $n_{po} = 50$, (b) $n_{po} = 100$, (c) $n_{po} = 200$ and (d) $n_{po} = 300$.

4. Results and discussion

Figure 6 shows the size distribution functions obtained with the model presented in equation (2) (dashed read line) in which the collision radius has been determined through the adjustment proposed in equation (7) with respect to

the experimental size distribution function obtained with the SMPS (solid blue line). As the equivalent diameter used in the modelled distribution is different to the electric mobility diameter obtained in the experimental distribution, the diameters of electric mobility have been corrected according to the approach explained in [17]. In the y-axis, the concentration of particles for a given size has been normalized with respect to the maximum value of the particle concentration. Therefore, the value of the distribution function is normalized with the value of the size distribution function at his mode.

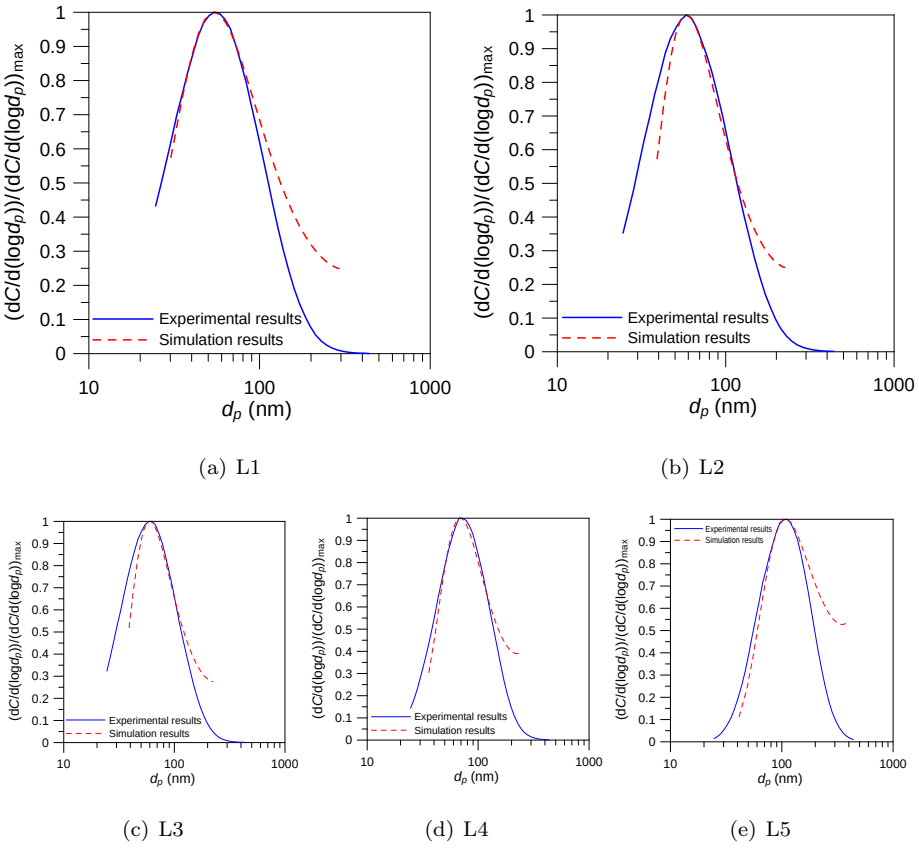

(a) L1 (b) L2

(c) L3 (d) L4 (e) L5

Figure 6: Size distribution functions for each operating point. (a) L1, (b) L2, (c) L3, (d) L4 and (e) L5.

Table 2 shows the relative error obtained when the modelled and experi-

mental size distribution modes are compared. The relative error obtained with the proposed semi-empirical model is lower than 3% for all tested engine operation modes, being lower than the uncertainty of the SMPS. The proposed model also reproduce the increase in the size distribution mode as a function of the increase in the engine load (Table 2), as well as the modelled particle size distributions are mono-modal coincident with these specific results and the majority of the experimental soot agglomerate size distributions [37]. However, as shown in figure 6, the size distribution function obtained with the proposed semi-experimental model is better suited to the experimental size distribution function for sizes less than 100 nm than for sizes larger than 100 nm.

Operating mode	d_{po} (nm)	d_{SMPS} (nm)	d_p (nm)	Relative error (%)
L1	21.36	54.25	54.71	0.85
L2	25.25	58.29	58.87	1.00
L3	26.87	62.64	61.08	2.49
L4	28.25	67.32	69.17	2.75
L5	29.26	111.40	108.96	2.19

Table 2: Modes obtained from the distribution functions for all test points.

It is well reported that agglomerate size distributions could be fitted to log-normal distributions [37]. Therefore, the modelled agglomerate size distributions are also fitted to log-normal distributions. A log-normal distribution is well defined with the mean $\overline{d_p}$ and standard deviation σ, equation (9). The mode of the modelled distribution function will be employed as the mean of the fitted log-normal distribution, while an empirical correlation based on the SMPS results is proposed to obtain the standard deviation.

$$f(d_p) = \frac{1}{\sqrt{2\pi}\ln(\sigma)} \exp\left[-\frac{1}{2\ln^2(\sigma)}\left(\ln(d_p) - \ln(\overline{d_p})\right)^2\right] \tag{9}$$

The SMPS results have been fitted to a log-normal size distribution. The fitting has been performed minimizing the mean quadratic error between the experimental and fitting values. Figure 7 and Table 3 compare the agglomerate

size distribution functions, mean diameter and standard deviation for the raw (directly obtained from the SMPS), and log-fitted experimental values at all the engine operation conditions. An empirical correlation has been found between the experimental mean diameter and standard deviation obtained from the log-normal fitting (Figure 8) and equation (10). The a, b and c coefficients of equation (10) has been obtained minimizing the mean quadratic error obtaining $a = 5.183 \times 10^8$, $b = -5.497$ and $c = 1.685$, being this fitting valid when $50 \leq \overline{d_p} \leq 115$.

$$\sigma = a\,\overline{d_p}^{\,b} + c \tag{10}$$

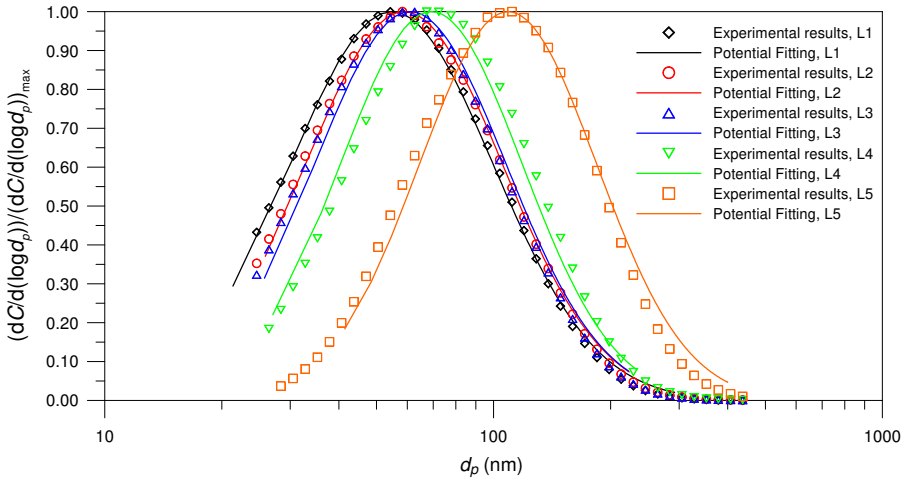

Figure 7: Comparison of agglomerate size distribution functions for all the engine operating conditions.

Operating mode	d_{SMPS} (nm)	$\overline{d_p}$ (nm)	σ
L1	54.25	54.71	1.825
L2	58.29	58.87	1.782
L3	62.64	61.08	1.764
L4	67.32	69.17	1.725
L5	111.10	108.96	1.688

Table 3: Experimental mean diameter and experimental log-normal fitting mean diameter and standard deviation

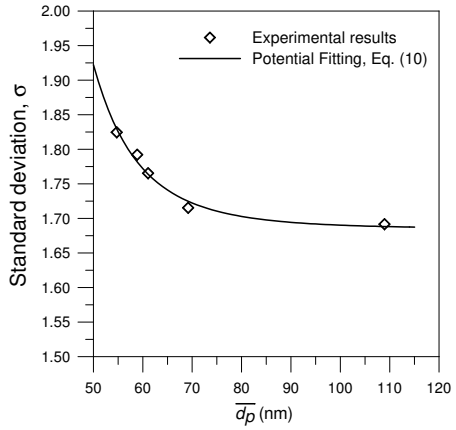

Figure 8: Empirical correlation between experimental mean diameter and standard deviation obtained from the log-normal fitting.

5. Conclusions

A semi-experimental model has been developed to obtain the agglomerate size distribution function emitted by a compression ignition engine fueled with standard diesel fuel. The model combines the attributes of phenomenological models utilising physically motivated relations for reliable extrapolation within some margins, with the computational efficiency and easiness to be handle of empirical models.

The required inputs of the model are constants as soot density, parameters as engine speed, air/fuel ratio, total volumetric soot concentration and mean instantaneous in-cylinder pressure, and empirical relations to obtain primary particle mean diameter and the relation between agglomerate size and number of primary particles, which compose the agglomerates. An acceptable fit has been obtained between the size distribution function obtained with the proposed model and the experimentally measured distribution function with a Scanning Mobility Particle Sizer (SMPS). The error made in the prediction of the mean particle size distribution is lower than the measurement error of the SMPS for all experimentally tested cases.

Acknowledgment

The authors express thanks to the University of Malaga for supporting through a thematic network. The authors would like to thank to the government of Spain (reference PRX15/00256) for providing a research stay to F.J. Martos at the University of Birmingham.

Appendix A. Nomenclature

A	air
d	diameter
C	soot concentration
D	diameter
F	fuel
i, j, k	size
L	lenght scale
n	number of particles
N	number of colissions
R	radius
Re	Reynolds number
s	engine speed

t	time
T	temperature
U	velocity
β	function of the collission frequency
η	Kolmogorov scale
ρ	density
ν	kinematic viscosity

Subscripts

i	index
j	index
p	particle
po	primary particle
s	soot

References

[1] V. Ramanathan, G. Carmichael, Global and regional climate changes due to black carbon, Nature Geoscience 1 (4) (2008) 221–227. doi:10.1038/ngeo156.

[2] A. Seaton, K. Donaldson, Nanoscience, nanotoxicology, and the need to think small, The Lancet 365 (9463) (2005) 923. doi:10.1016/S0140-6736(05)71061-8.

[3] 2008/692/EC, Implementing and amending Regulation (EC) No 715/2007 of the European Parliament and of the Council on type-approval of motor vehicles with respect to emissions from light passenger and commercial vehicles (Euro 5 and Euro 6) and on access to vehicle repair and maintenance information.

[4] K. E. Lehtinen, M. R. Zachariah, Energy accumulation in nanoparticle collision and coalescence processes, Journal of Aerosol Science 33 (2) (2002) 357–368. doi:10.1016/S0021-8502(01)00177-X.

[5] J.-O. Müller, D. S. Su, R. E. Jentoft, U. Wild, R. Schlögl, Diesel engine exhaust emission: Oxidative behavior and microstructure of black smoke soot particulate, Environmental Science & Technology 40 (4) (2006) 1231–1236. doi:10.1021/es0512069.

[6] P. A. Bonczyk, R. J. Hall, Fractal properties of soot agglomerates, Langmuir 7 (6) (1991) 1274–1280. doi:10.1021/la00054a042.

[7] P. Meakin, Fractal aggregates, Advances in Colloid and Interface Science 28 (1987) 249–331. doi:10.1016/0001-8686(87)80016-7.

[8] C. Sorensen, The mobility of fractal aggregates: a review, Aerosol Science & Technology 45 (7) (2011) 765–779. doi:10.1080/02786826.2011.560909.

[9] G. Wang, C. Sorensen, Diffusive mobility of fractal aggregates over the entire Knudsen number range, Physical Review E 60 (3) (1999) 3036. doi:10.1103/PhysRevE.60.3036.

[10] E. Knutson, K. Whitby, Aerosol classification by electric mobility: apparatus, theory, and applications, Journal of Aerosol Science 6 (6) (1975) 443–451. doi:10.1016/0021-8502(75)90060-9.

[11] S. Z. Rezaei, F. Zhang, H. Xu, A. Ghafourian, J. M. Herreros, S. Shuai, Investigation of two-stage split-injection strategies for a Dieseline fuelled PPCI engine, Fuel 107 (2013) 299–308. doi:10.1016/j.fuel.2012.11.048.

[12] M. Bogarra, J. Martin, C. H. Herreros, A. Tsolakis, A. P. York, J. Paul, Influence of three-way catalyst on gaseous and particulate matter emissions during gasoline direct injection engine cold-start. analysing emissions to

meet Euro6c legislation, Johnson Matthey's International Journal of Research Exploring Science and Technology in Industrial Applications (2017) 329doi:10.1595/205651317x696315.

[13] O. Armas, A. Gómez, J. Herreros, Uncertainties in the determination of particle size distributions using a mini tunnel–SMPS system during diesel engine testing, Measurement Science and Technology 18 (7) (2007) 2121. doi:10.1088/0957-0233/18/7/044.

[14] S. Park, S. Rogak, A one-dimensional model for coagulation, sintering, and surface growth of aerosol agglomerates, Aerosol Science & Technology 37 (12) (2003) 947–960. doi:10.1080/02786820300899.

[15] M. Mueller, G. Blanquart, H. Pitsch, Hybrid method of moments for modeling soot formation and growth, Combustion and Flame 156 (6) (2009) 1143–1155. doi:10.1016/j.combustflame.2009.01.025.

[16] M. E. Mueller, G. Blanquart, H. Pitsch, A joint volume-surface model of soot aggregation with the method of moments, Proceedings of the Combustion Institute 32 (1) (2009) 785–792. doi:10.1016/j.proci.2008.06.207.

[17] M. Lucchesi, A. Abdelgadir, A. Attili, F. Bisetti, Simulation and analysis of the soot particle size distribution in a turbulent nonpremixed flame, Combustion and Flame 178 (2017) 35–45. doi:10.1016/j.combustflame.2017.01.002.

[18] N. A. Henein, Analysis of pollutant formation and control and fuel economy in diesel engines, Progress in Energy and Combustion Science 1 (4) (1976) 165–207. doi:10.1016/0360-1285(76)90013-7.

[19] J. E. Dec, A conceptual model of DI diesel combustion based on laser-sheet imaging, Tech. rep., SAE Technical paper (1997). doi:10.4271/970873.

[20] B. Liu, J. Hu, F. Yan, R. F. Turkson, F. Lin, A novel optimal support vector machine ensemble model for NO_x emissions prediction of a diesel

engine, Measurement 92 (2016) 183–192. doi:10.1016/j.measurement.2016.06.015.

[21] J. Asprion, O. Chinellato, L. Guzzella, A fast and accurate physics-based model for the NO_x emissions of diesel engines, Applied Energy 103 (2013) 221–233. doi:10.1016/j.apenergy.2012.09.038.

[22] M. Warth, P. Obrecht, A. Bertola, K. Boulouchos, Predictive phenomenological CI Combustion modeling optimization on the basis of bio-inspired algorithms, Tech. rep., SAE Technical Paper (2005). doi:10.4271/2005-01-1119.

[23] S. Aithal, D. Upadhyay, Feasibility study of the potential use of chemistry based emission predictions for real-time control of modern diesel engines, Applied Energy 91 (1) (2012) 475–482. doi:10.1016/j.apenergy.2011.10.005.

[24] C. Ericson, B. Westerberg, I. Odenbrand, R. Egnell, Characterisation and model based optimization of a complete diesel engine/SCR system, Tech. rep., SAE Technical Paper (2009). doi:10.4271/2009-01-0896.

[25] I. Motroniuk, R. Królak, R. Stöber, G. Fischerauer, Wireless communication-based state estimation of automotive aftertreatment systems, Measurement 106 (2017) 245–250. doi:10.1016/j.measurement.2016.08.004.

[26] J. Heywood, Internal combustion engine fundamentals, McGraw-Hill Education, 1988.

[27] U. Asad, R. Kumar, X. Han, M. Zheng, Precise instrumentation of a diesel single-cylinder research engine, Measurement 44 (7) (2011) 1261–1278. doi:10.1016/j.measurement.2011.03.028.

[28] P. D. Kinney, D. Y. Pui, G. W. Mulliolland, N. P. Bryner, Use of the electrostatic classification method to size 0.1 μm srm particles—a feasibil-

ity study, Journal of Research of the National Institute of Standards and Technology 96 (2) (1991) 147. doi:10.6028/jres.096.006.

[29] N. A. Fuchs, The mechanics of aerosols, Dover Publications, 1989. doi:10.1002/qj.49709138822.

[30] F. J. Martos, M. Lapuerta, J. J. Expósito, E. Sanmiguel-Rojas, Overestimation of the fractal dimension from projections of soot agglomerates, Powder Technology 311 (2017) 528–536. doi:10.1016/j.powtec.2017.02.011.

[31] S. K. Friedlander, Smoke, Dust, and Haze: Fundamentals of Aerosol Dynamics, Oxford University Press, New York, 2000.

[32] S. B. Pope, Turbulent Flows, Cambridge University press, 2000. doi:10.1017/CBO9780511840531.

[33] J. Heywood, Combustion and its modeling in spark-ignition engines, International Symposium COMODIA 94 (1994) 1–15.

[34] J. Cai, C. Sorensen, Diffusion of fractal aggregates in the free molecular regime, Physical Review E 50 (5) (1994) 3397. doi:10.1103/PhysRevE.50.3397.

[35] M. Lapuerta, O. Armas, J. Hernández, Diagnosis of DI Diesel combustion from in-cylinder pressure signal by estimation of mean thermodynamic properties of the gas, Applied Thermal Engineering 19 (5) (1999) 513–529. doi:10.1016/S1359-4311(98)00075-1.

[36] M. Lapuerta, F. J. Martos, J. M. Herreros, Effect of engine operating conditions on the size of primary particles composing diesel soot agglomerates, Journal of Aerosol Science 38 (4) (2007) 455–466. doi:10.1016/j.jaerosci.2007.02.001.

[37] D. B. Kittelson, Engines and nanoparticles: a review, Journal of Aerosol Science 29 (5) (1998) 575–588. doi:10.1016/S0021-8502(97)10037-4.